Supporting Information

Synthesis of 5,5'-azoxybistetrazole via nitration and de-oxygen rearrangement of triazene

Qi Wang,[a] Tian Lu,[a] Chenbin Wang,[a] Guijuan Fan,[b] Hongquan Yin,[a] and Fu-Xue Chen[a]*

a School of Chemistry & Chemical Engineering, Beijing Institute of Technology, Beijing 100081, China
b Institute of Chemical Materials, China Academy of Engineering Physics, Mianyang, 621050, Sichuan, China.
fuxue.chen@bit.edu.cn

Contents

Optimization of reaction condition to synthesize 2a

Besides acetic anhydride, the deoxidizing agent with lower electron densities (Table S1, entry 1 and 2) has a negative effect on the yield. In addition, more active de-oxygen agents, such as triethyl phosphite and oxalyl chloride (entry 3 and 4), produce no product might due to excessive reduction of nitro triazene intermediate.

Table S1. Synthesis of **2a** using different de-oxygen reagent.[a]

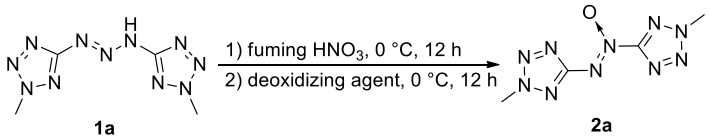

1a **2a**

entry	deoxidizing agent	Yield (%)[b]
1	$(PhCO)_2O$	24
2	$(CF_3CO)_2O$	6
3	$P(OEt)_3$	0
4	$(COCl)_2$	0

[a] Reactions were carried out with (1) 1,3-bis(2-methyltetrazol-5-yl)triazene (**1a**, 0.5 mmol) in fuming HNO_3 and (2) deoxidizing agent. [b] Isolated yield.

Investigations of mechanism

When **1d** and **1e** were mixed of 1:1 ratio as starting material, cross-reacted product **2de** and **2ed** were not observed in mass spectrum (Scheme **S1**), which indicated that the product was formed via intramolecular rearrangement rather than cleavage followed by combination.

Scheme S1. Cross-reaction of two different substituted tetrazolyl triazenes

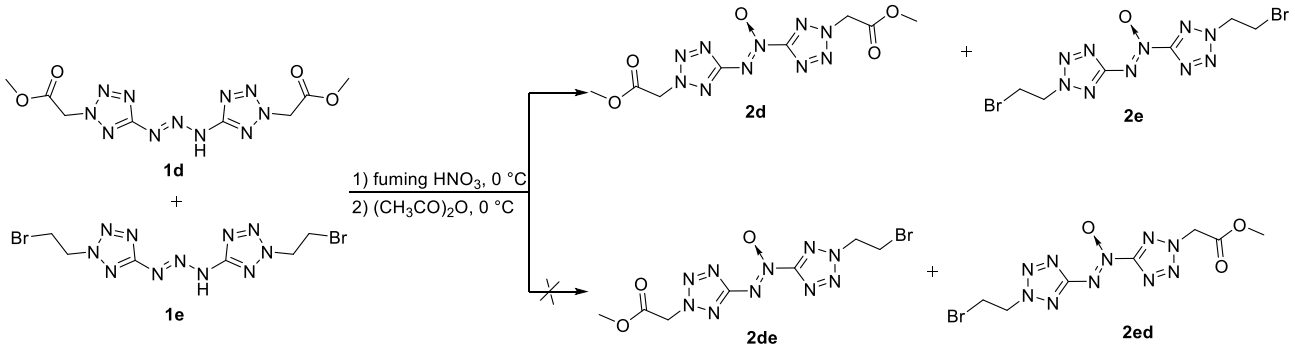

Caution! Due to the fact that 5,5'-azoxybistetrazoles are to some extent rather unstable toward external stimuli, proper safety precautions should be taken when handling the dry materials. Lab personnel and the equipment should be properly grounded and protective equipment such as leather coat, Kevlar gloves, ear protection and face shield are recommended.

General Methods: ^{1}H and ^{13}C NMR spectra were recorded on a 400 MHz (Buruker Avance 400) nuclear magnetic resonance spectrometers operating at 400 and 100 MHz, respectively, by using DMSO-D_6 as solvent and locking solvent. ^{15}N NMR spectra were recorded on a 700 MHz (Buruker Avance 700) nuclear magnetic resonance spectrometers operating at 70 MHz by using DMSO-D_6 as solvent and locking solvent. IR spectra were recorded using KBr pellets for solids on a Bruker ALPHA FT-IR-Spektrometer. The melting and decomposition points were obtained on a differential scanning calorimeter (METTLER TOLEDO) at a scan rate of 5 ºC·min^{-1}. Elemental analyses were carried out using an Elementar Vario EL element alanalyzer. High resolution mass spectrometry was recorded on Bruker Apex IV FTMS.

X-ray diffraction: For compound **2a**, data were collected on a Rigaku Saturn 724 CCD diffractometer employing graphite-monochromated MoKa radiation (λ=0.71073 Å) using omega scans. Data collection and reduction were performed and the unit cell was initially refined using Crystal Clear SM Expert 2.0 r2.[1] The reflection data were corrected for Lorentz-polarization factors. The structure was solved by direct methods and refined by the least-squares method on F^2 using the SHELXTL-97 suite of programs.[2] All non-hydrogen atoms were refined an isotropically. The structure of **2a** was solved in the space group $P2_1/c$ by analysis of systematic absences.

Compound **1a-1f** were synthesized according as literature.[3]

2,2'-dimethyl-5,5'-azoxybistetrazole (2a). Yield 56 mg (53%) of product **2a**.

White solid (**2a**): DSC (5 °C·min^{-1}): 162 °C (m.p.); 183 °C (dec.). IR (KBr): $\tilde{\nu}$ = 3050, 1513, 1491, 1449, 1406, 1288, 1197, 1071, 1032, 1023, 916, 805, 749 cm^{-1}; ^{1}H NMR (400 MHz, DMSO-d_6): δ = 4.55 (s, 3H, CH_3), 4.50 (s, 3H, CH_3) ppm. ^{13}C NMR (100 MHz, DMSO-d_6): δ = 165.5, 162.9, 41.1, 40.3 ppm; ^{15}N NMR (70 MHz, DMSO-d_6): δ = 4.8 (N9), -0.4 (N3), -50.1 (N10), -57.8 (N4), -70.1 (N7), -74.0 (N1), -79.0 (N5), -79.6 (N6), -98.2 (N8), -102.0 (N2) ppm; HRMS: calc. for $C_4H_6N_{10}O$ $[M+Na]^+$: 233.0618; found: 233.0613. Elemental analysis: ($C_4H_6N_{10}O$, 210.16) calc.: C 22.86, H 2.88, N 66.65; found: C 23.17, H 2.75, N 66.47.

2,2'-di(*tert*-butyl)-5,5'-azoxybistetrazole (2b). Yield 92 mg (63%) of product **2b**.

White solid (**2b**): m.p.: 120-121 °C. ^{1}H NMR (400 MHz, DMSO-d_6): δ = 1.79 (s, 9H, CH_3), 1.76 (s, 9H, CH_3) ppm. ^{13}C NMR (100 MHz, DMSO-d_6): δ = 165.3, 162.7, 66.8, 65.2, 28.6, 28.5 ppm; HRMS: calc. for $C_{10}H_{18}N_{10}O$ $[M+ Na]^+$: 317.1557; found: 317.1557.

2,2'-di(cyanomethyl)-5,5'-azoxybistetrazole (2c). Yield 98 mg (76%) of product **2c**.

White solid (**2c**): DSC (5 °C·min^{-1}): 182 °C (dec.). $\tilde{\nu}$ = 2981, 2944, 1518, 1491, 1427, 1414, 1389, 1347, 1031, 955, 919, 798 cm^{-1}; ^{1}H NMR (400 MHz, DMSO-d_6): δ = 6.46 (s, 2H, CH_2), 6.40 (s, 2H, CH_2) ppm. ^{13}C NMR (100 MHz, DMSO-d_6): δ = 165.7, 163.2, 113.2, 112.8, 42.3, 41.5 ppm; HRMS: calc. for $C_6H_4N_{12}O$ $[M-H]^-$: 259.0558; found: 259.0557.

2,2'-di(methoxycarbonylmethyl)-5,5'-azoxybistetrazole (2d). Yield 124 mg (76%) of product **2d**.

White solid (**2d**): m.p.: 133-134 °C. IR (KBr): $\tilde{\nu}$ = 3010, 2967, 1747, 1514, 1496, 1442, 1415, 1357, 1244, 988, 911, 825 cm^{-1}; ^{1}H NMR (400 MHz, DMSO-d_6): δ = 6.12 (s, 2H, CH_2), 6.04 (s, 2H, CH_2), 3.79 (s, 3H, CH_3), 3.77 (s, 3H, CH_3) ppm. ^{13}C NMR (100 MHz, DMSO-d_6): δ = 166.8, 166.3, 166.3, 163.7, 55.3, 54.5, 53.7, 53.6 ppm; HRMS: calc. for $C_8H_{10}N_{10}O_5$ $[M+H]^+$: 327.0908; found: 327.0904.

2,2'-di(bromoethyl)-5,5'-azoxybistetrazole (2e). Yield 158 mg (80%) of product **2e**.

White solid (**2e**): m.p.: 124-125 °C. IR (KBr): $\tilde{\nu}$ = 3034, 3004, 2976, 1513, 1491, 1438, 1416, 1391, 1359, 1303, 1275, 955, 915, 883, 784 cm^{-1}; ^{1}H NMR (400 MHz, DMSO-d_6): δ = 5.35 (t, *J*=5.6 Hz, 2H, *N*-CH_2), 5.29 (t, *J*=5.6 Hz, 2H, *N*-CH_2), 4.11 (t, *J*=5.6 Hz, 2H, *Br*-CH_2), 4.09 (t, *J*=5.6 Hz, 2H, *Br*-CH_2) ppm. ^{13}C NMR (100 MHz, DMSO-d_6): δ = 165.6, 163.1, 55.9, 55.0, 29.8, 29.3 ppm; HRMS: calc. for $C_6H_8Br_2N_{10}O$ $[M+H]^+$: 394.9322; found: 394.9320.

2,2'-di(hydroxyethyl)-5,5'-azoxybistetrazole dinitrate (2f). Yield 148 mg (82%) of product **2f**.

White solid (**2f**): DSC (5 °C·min^{-1}): 114 °C (m.p.); 175 °C (dec.). IR (KBr): $\tilde{\nu}$ = 3035, 2985, 2909, 1636, 1522, 1507, 1457, 1420, 1384, 1284, 1028, 893, 861 cm^{-1}; ^{1}H NMR (400 MHz, DMSO-d_6): δ = 5.34 (s, 2H, *N*-CH_2), 5.29 (s, 2H, *N*-CH_2), 5.12 (s, 4H, *O*-CH_2) ppm. ^{13}C NMR (100 MHz, DMSO-d_6): δ = 165.7, 163.2, 70.2, 69.9, 52.0, 51.2 ppm; ^{15}N NMR (70 MHz, DMSO-d_6): δ = 5.6 (N9), 0.3 (N3), -43.5 (N12), -43.6 (N11), -49.2 (N10), -56.6 (N4), -69.9 (N7), -74.3 (N1), -80.3 (N5), -80.6 (N6), -95.3 (N8), -98.9 (N2) ppm; HRMS: calc. for $C_6H_8N_{12}O_7$ $[M+H]^+$: 361.0712; found: 361.0712.

2,2'-di(azidoethyl)-5,5'-azoxybistetrazole (**2g**) Yield 105 mg (30%) of product **2g**.

White solid (**2g**): DSC (5 °C·min^{-1}): 102 °C (m.p.); 189 °C (dec.). IR (KBr): $\tilde{\nu}$ = 2937, 2136, 2099, 1512, 1490, 1442, 1418, 1347, 1284, 1244, 1014, 914, 788, 748 cm^{-1}; ^{1}H NMR (400 MHz, DMSO-d_6): δ = 5.09 (t, *J*=5.4 Hz, 2H, *Tr*-CH_2), 5.04 (t, *J*=5.0 Hz, 2H, *Tr*-CH_2), 4.06 (t, *J*=5.2 Hz, 2H, N_3-CH_2), 4.02 (t, *J*=5.2 Hz, 2H, N_3-CH_2) ppm; ^{13}C NMR (100 MHz, DMSO-d_6): δ = 165.6, 163.1, 53.8, 52.9, 48.9, 48.6 ppm; HRMS: calc. for $C_6H_8N_{16}O$ $[M+H]^+$: 321.1140; found: 321.1139. Elemental analysis: ($C_6H_8N_{16}O$, 320.11) calc.: C 20.01, H 2.24, N 46.66; found: C 20.60, H 2.13, N 46.18.

References

1 *CrystalClear: SM Expert 2.0 r2, An Integrated Program for the Collection and Processing of Area Detector Data*, Rigaku Corporation, England, **2009**.

2 G. M. Sheldrick, *SHELXTL-97, Structure Determination Software Suite*, Bruker AXS, Madison, **2008**.

3 Wang, Q.; Pang, F.; Wang, G.; Huang, J.; Nie, F.; Chen, F.-X. *Chem. Commun.* **2017**, *53*, 2327–2330.

X-ray crystallography of 2a

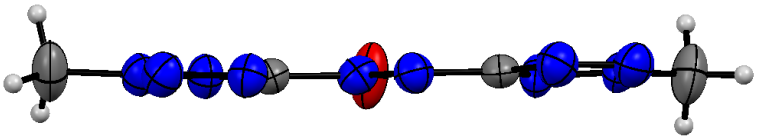

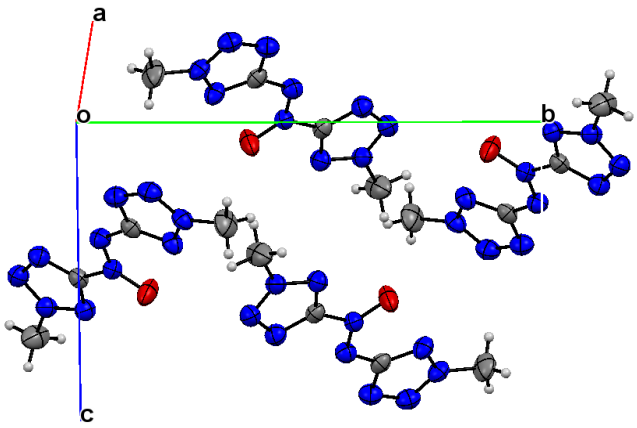

Spectral data of 2a

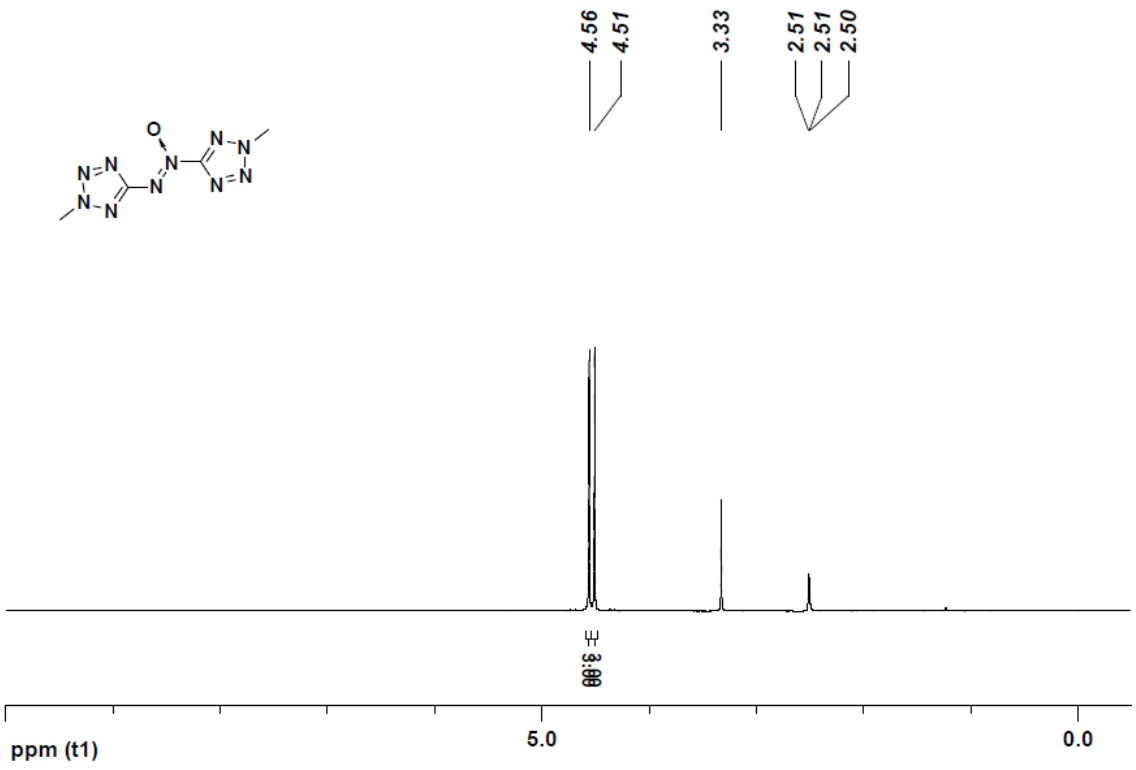

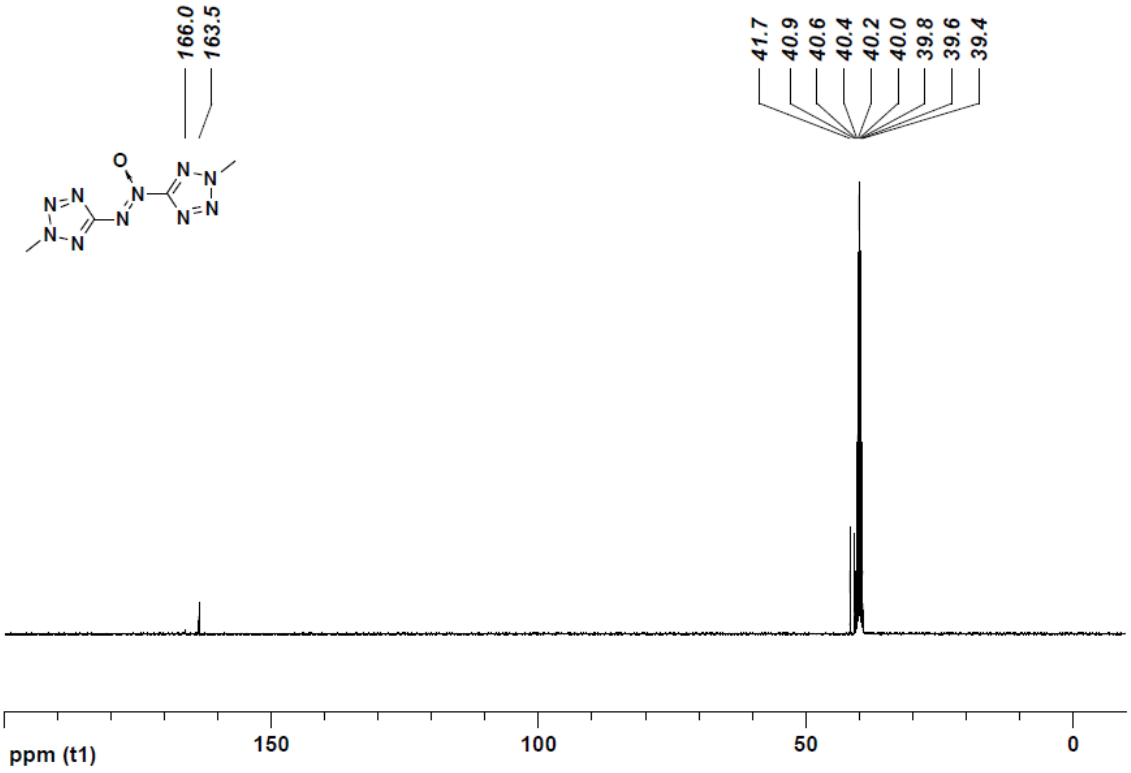

Infrared

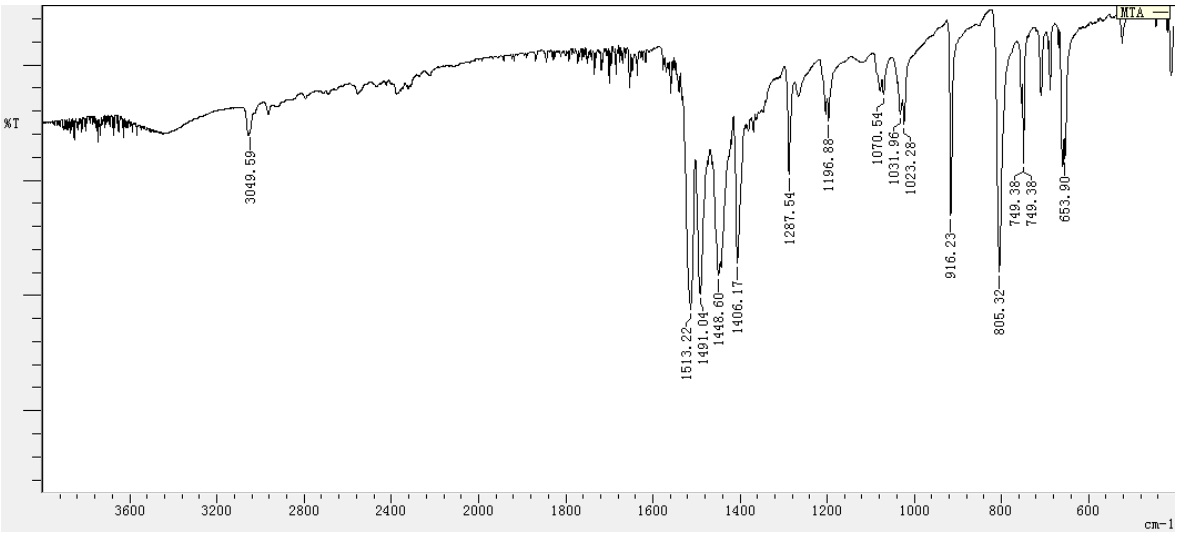

HRMS

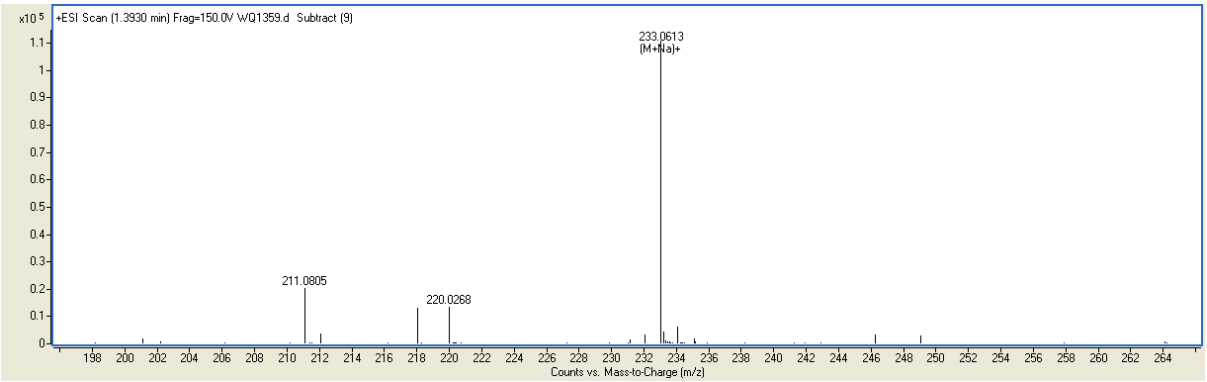

DSC

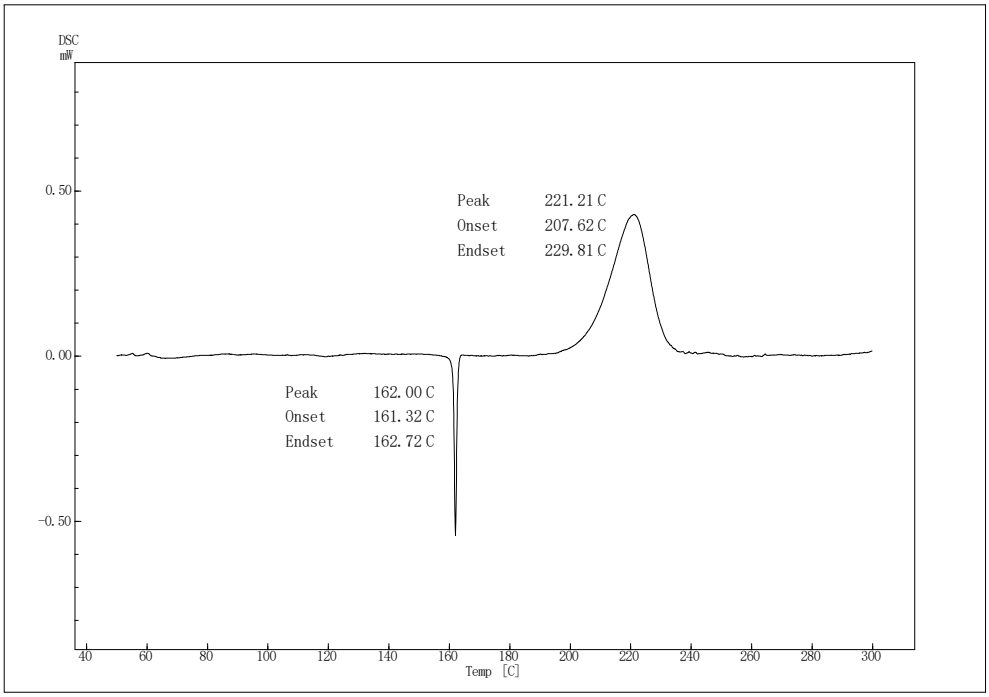

Spectral data of 2b

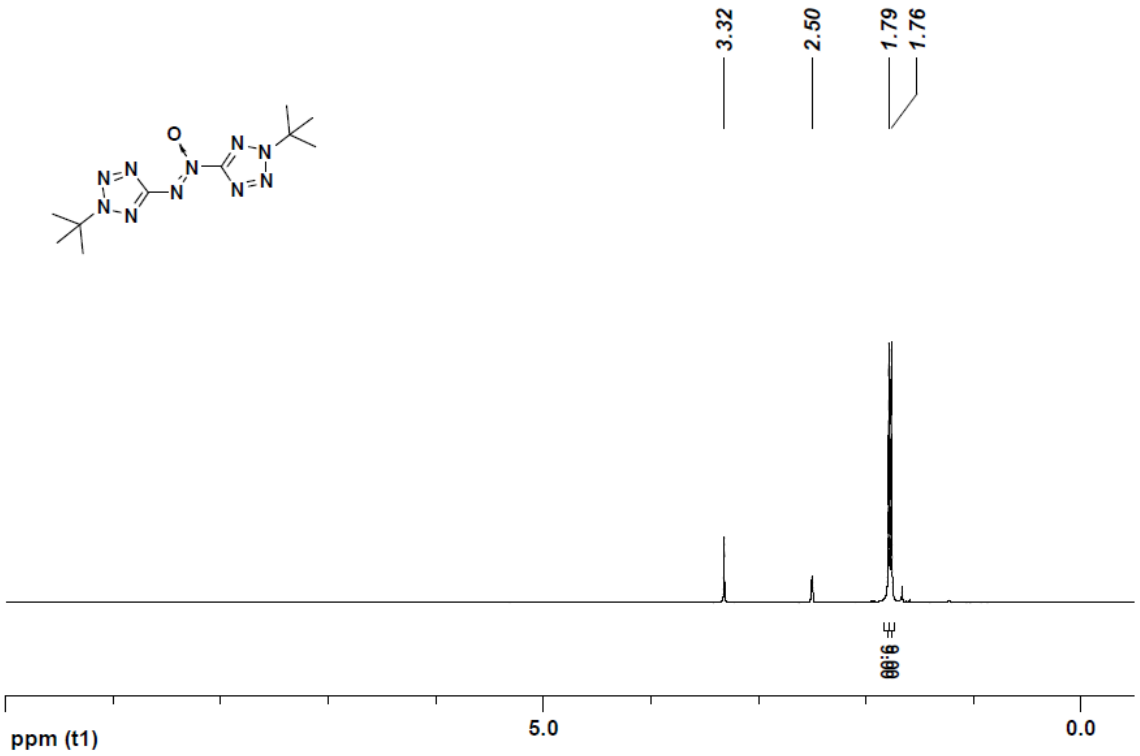

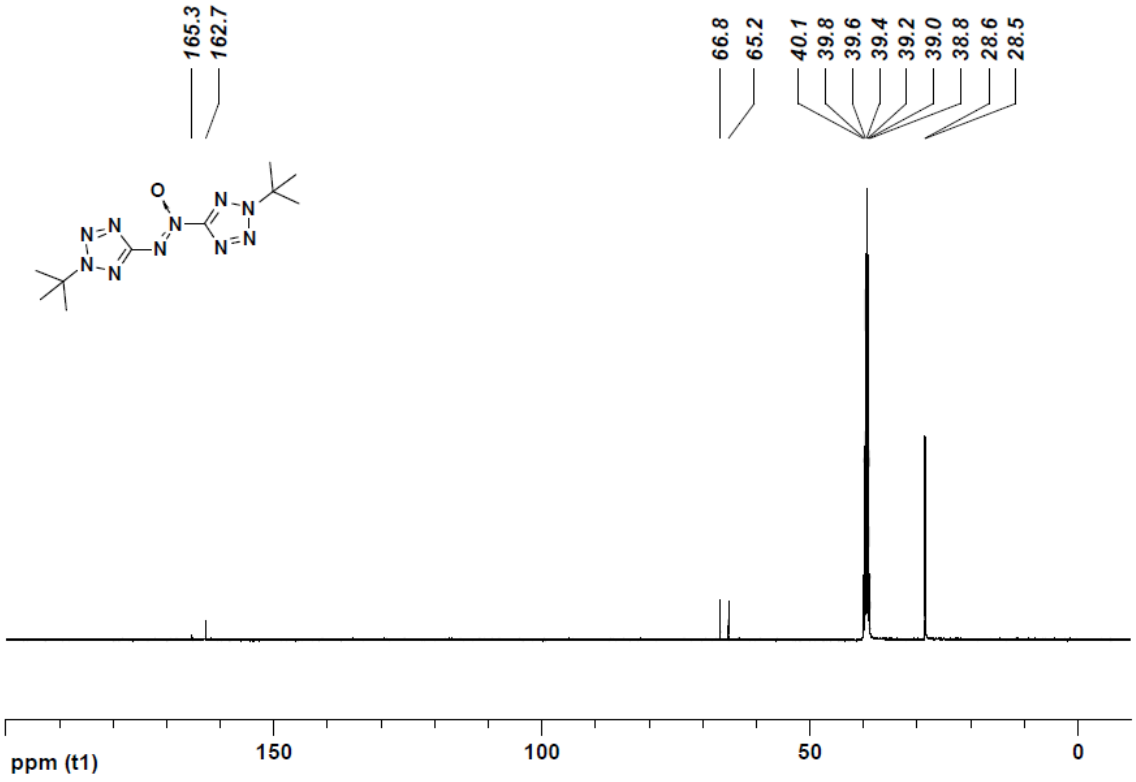

HRMS

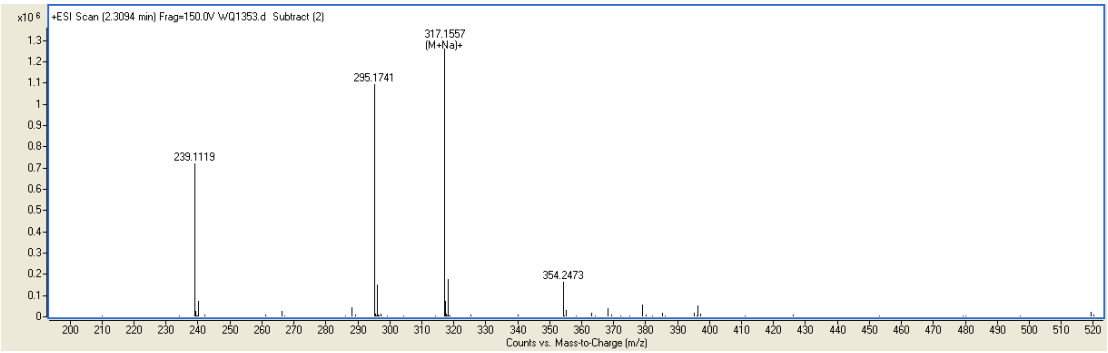
+ESI Scan (2.3094 min) Frag=150.0V WQ1353.d Subtract (2)
x10 6
317.1557
(M+Na)+
295.1741
239.1119
354.2473
Counts vs. Mass-to-Charge (m/z)

Spectral data of 2c

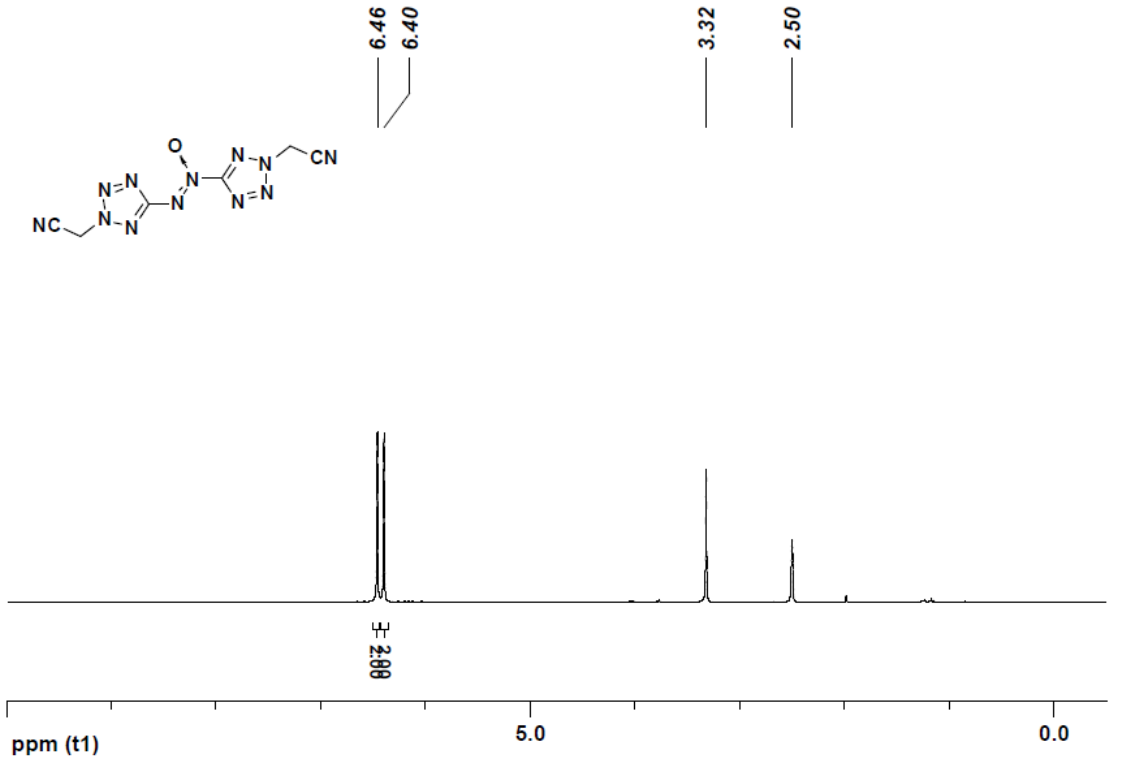

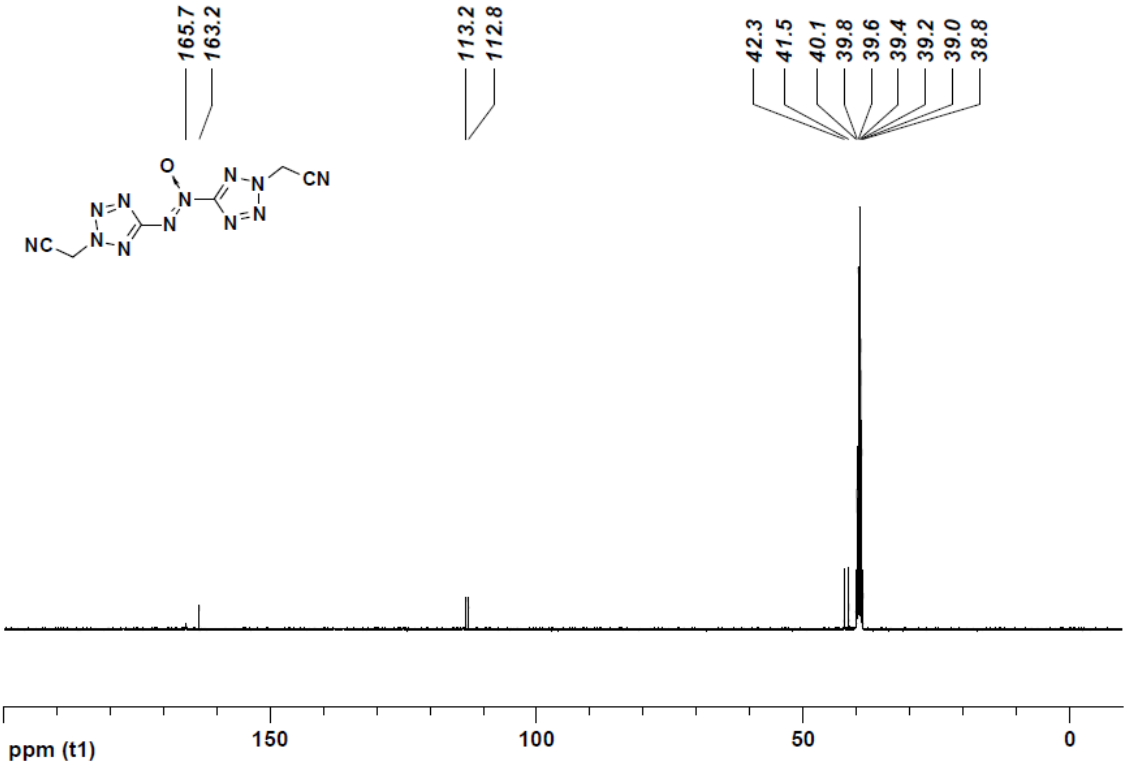

Infrared

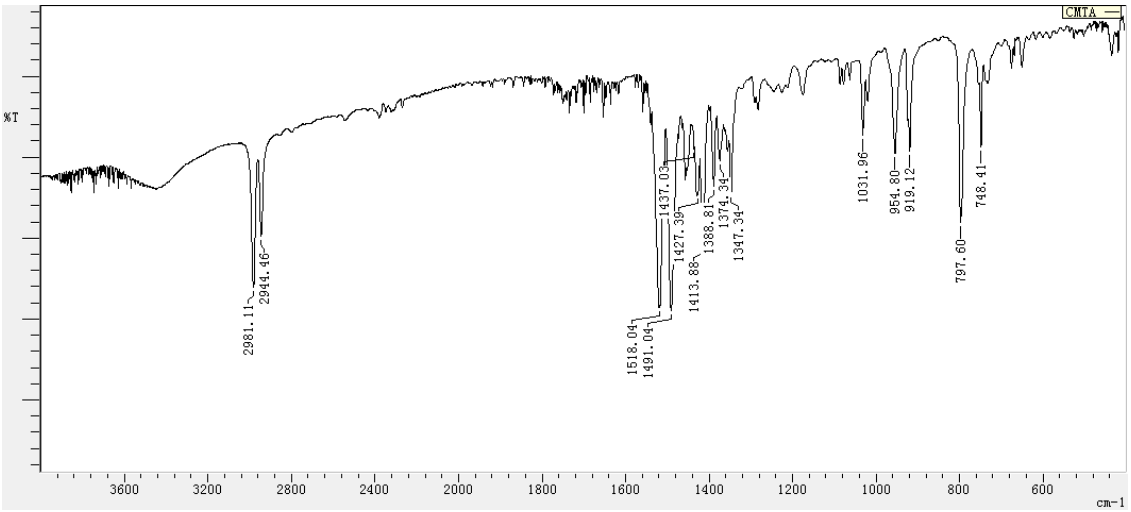

HRMS

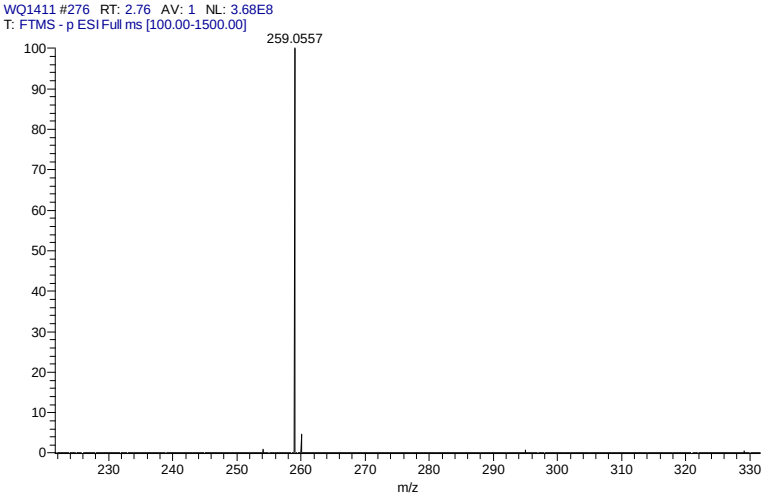

DSC

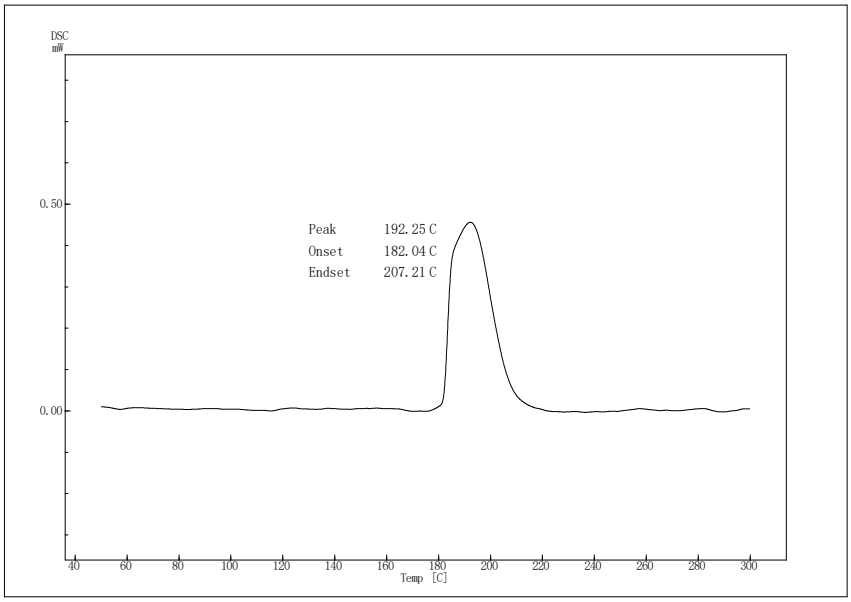

Spectral data of 2d

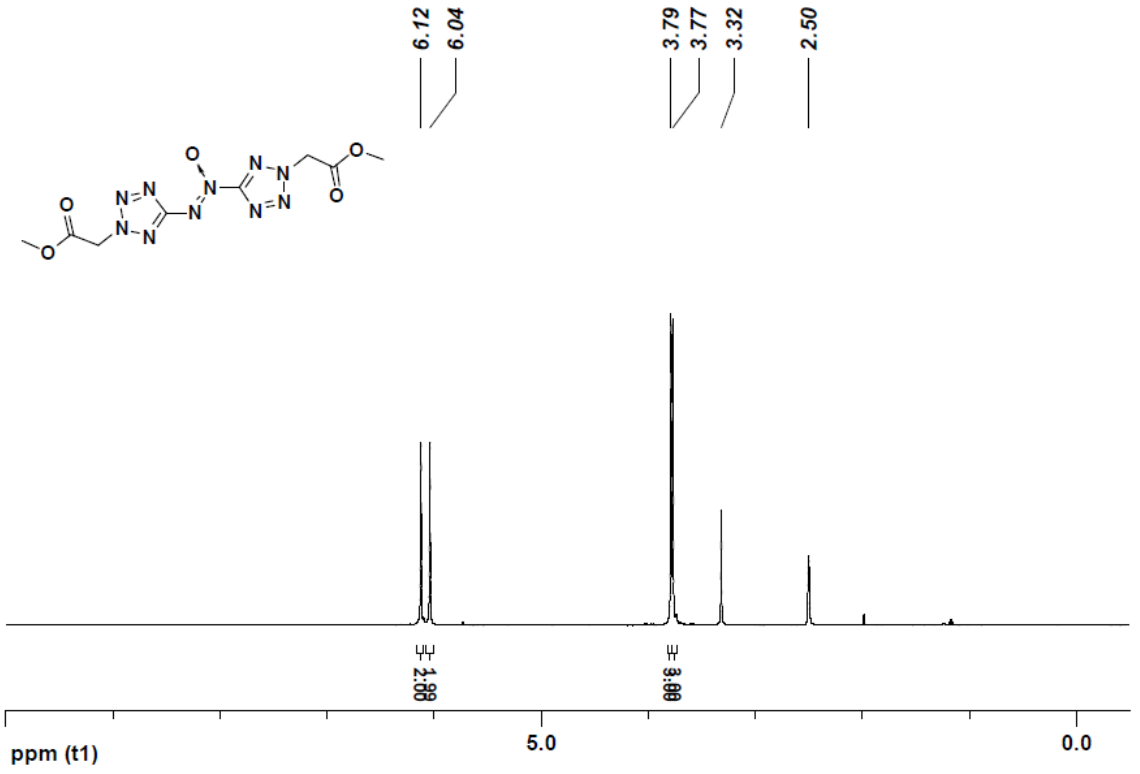

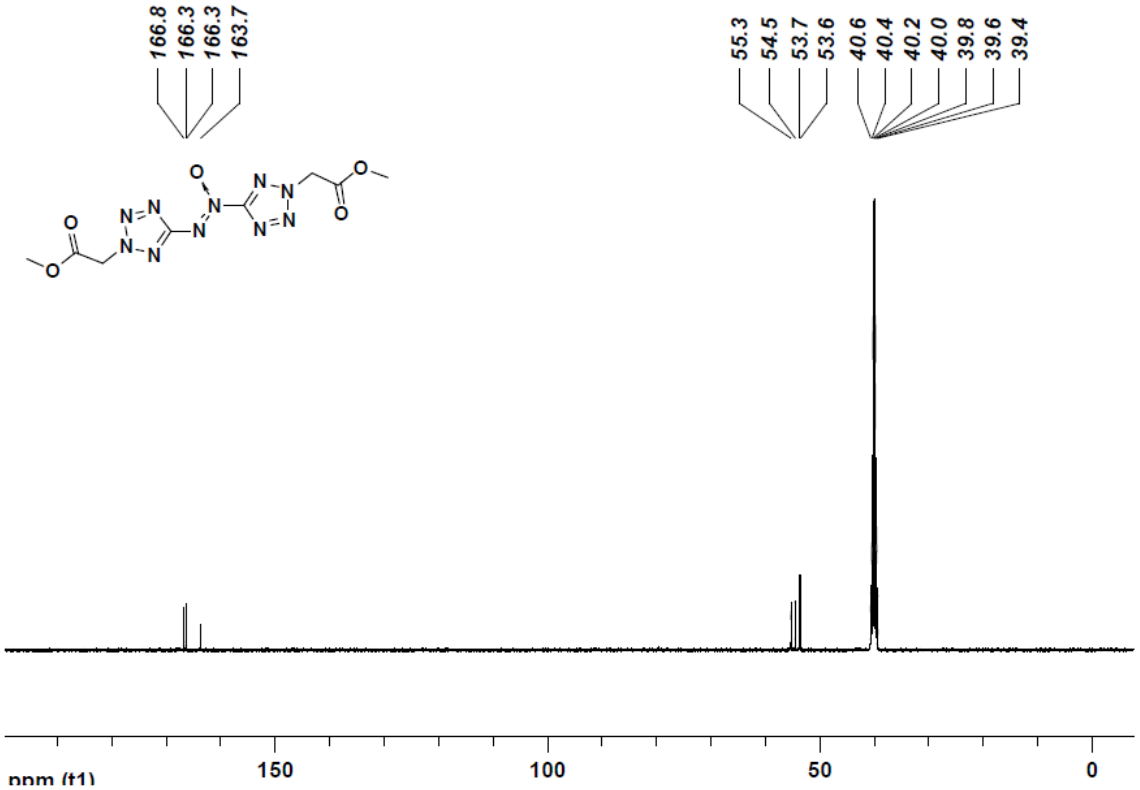

Infrared

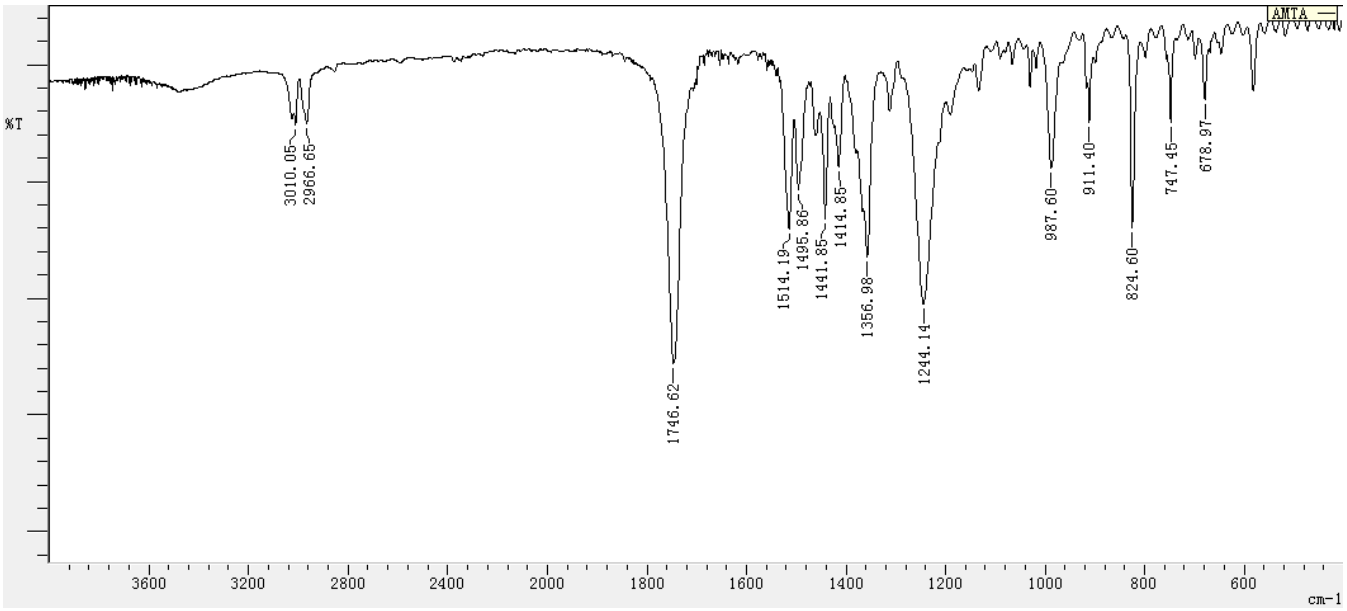

HRMS

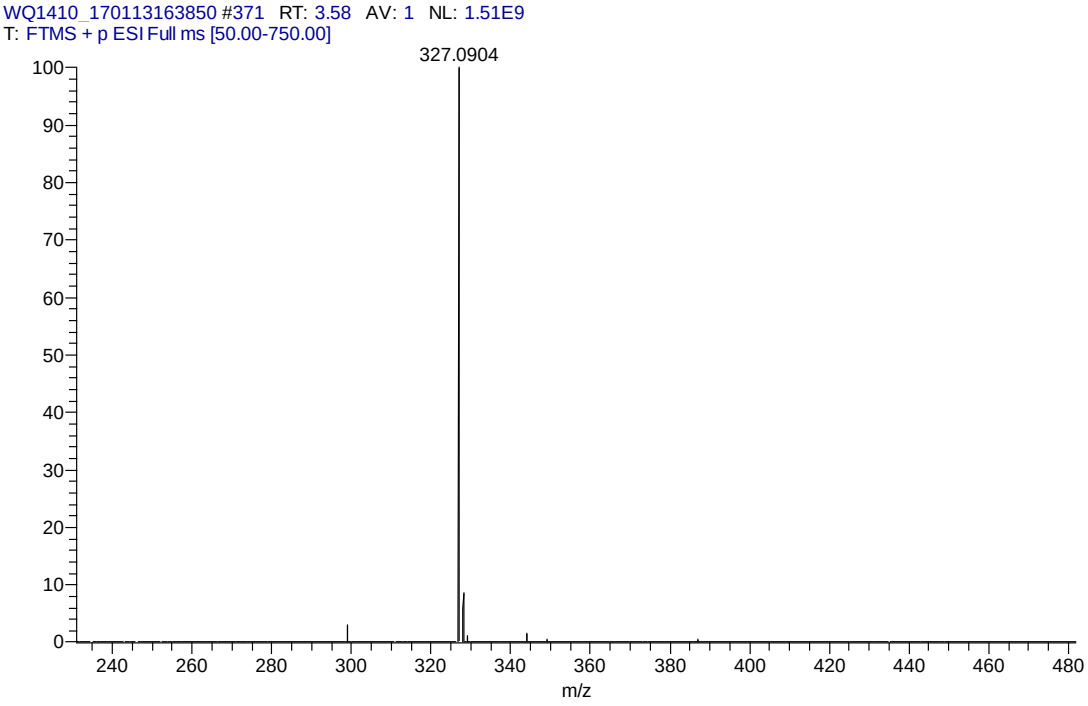

Spectral data of 2e

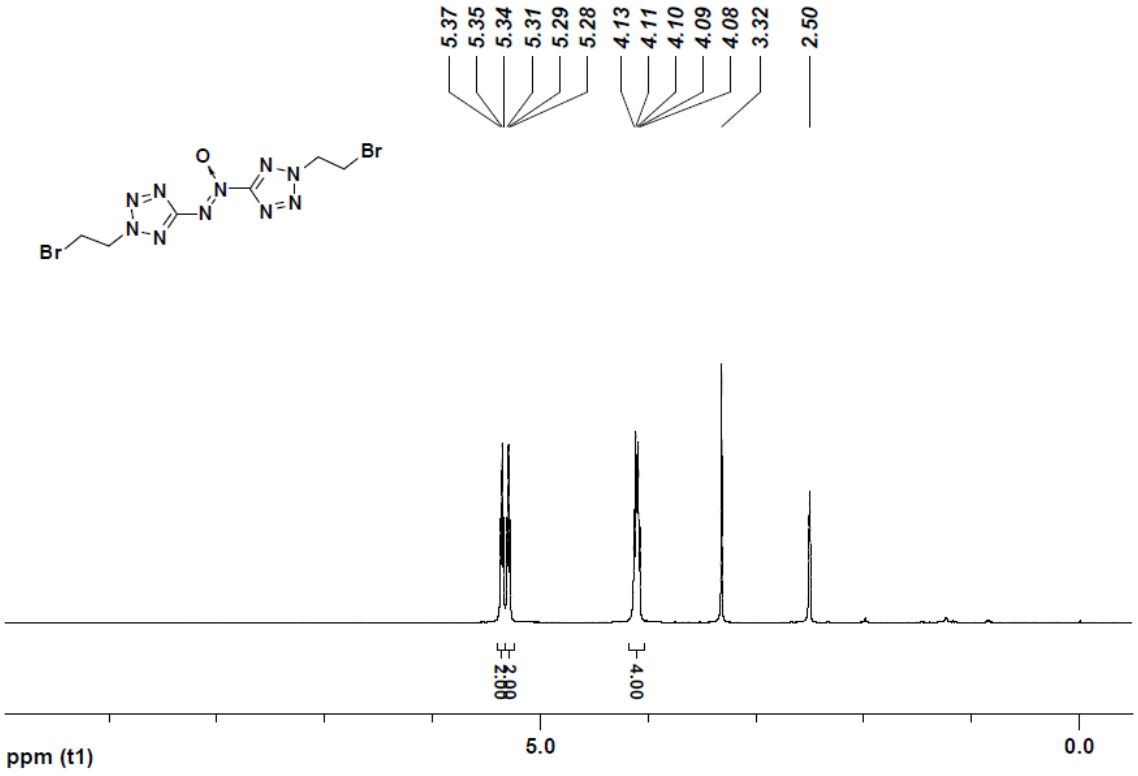

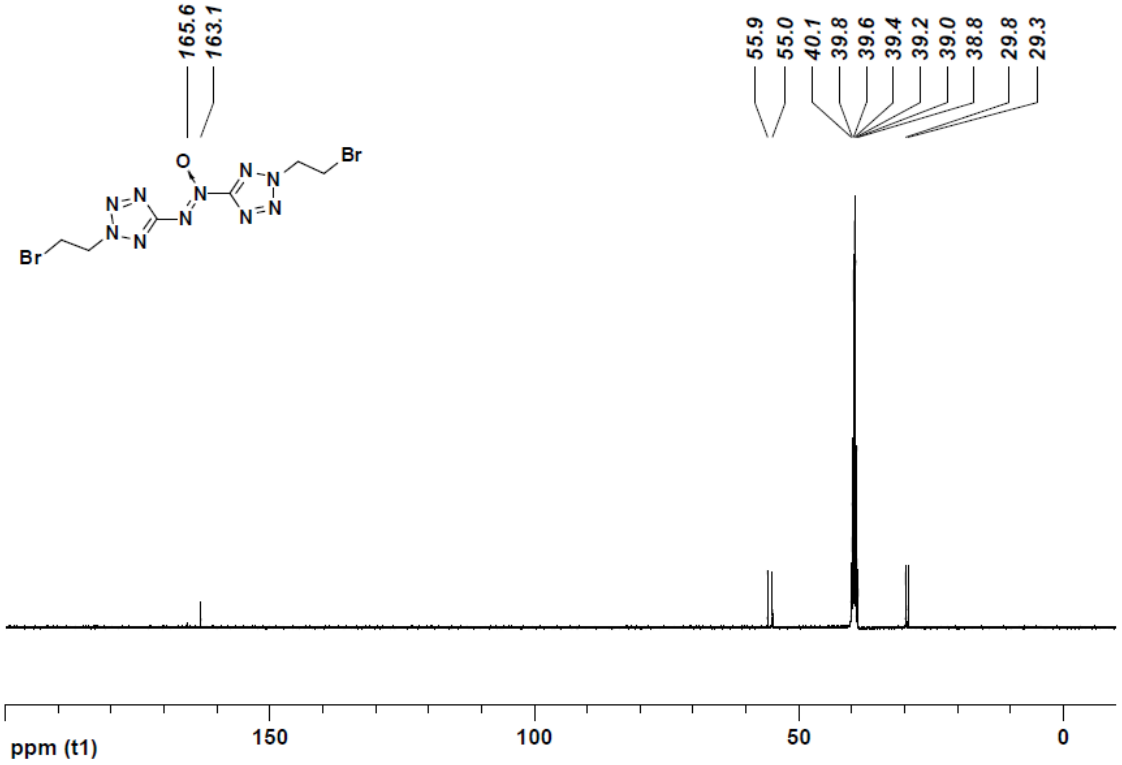

Infrared

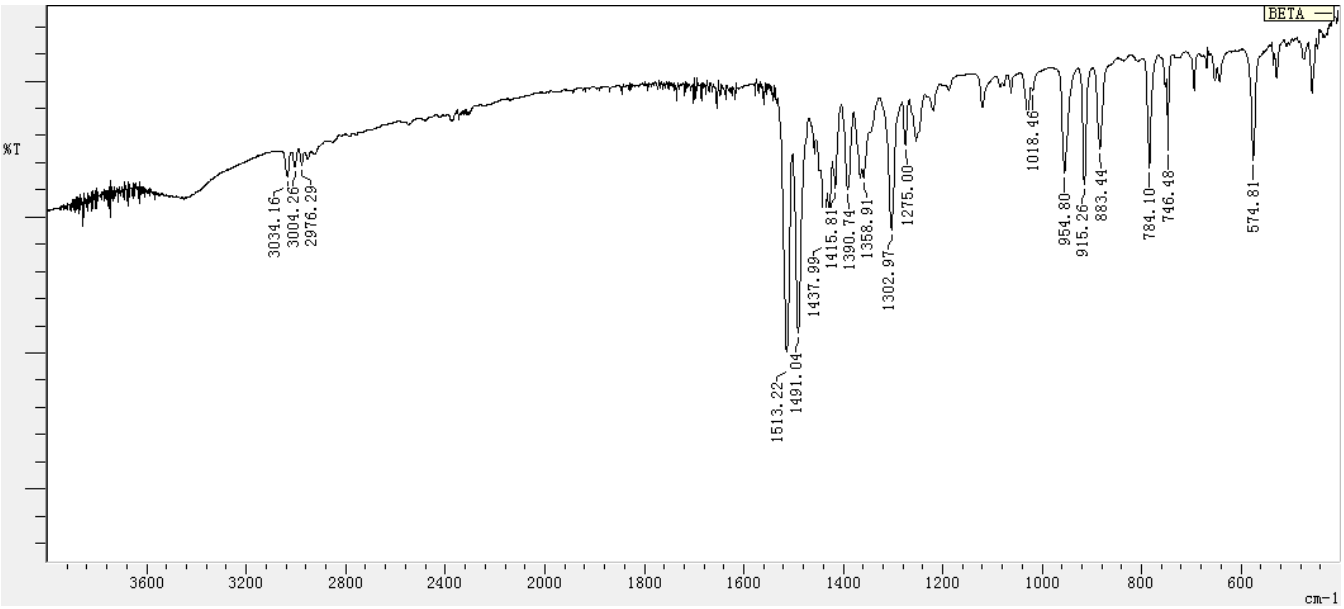

HRMS

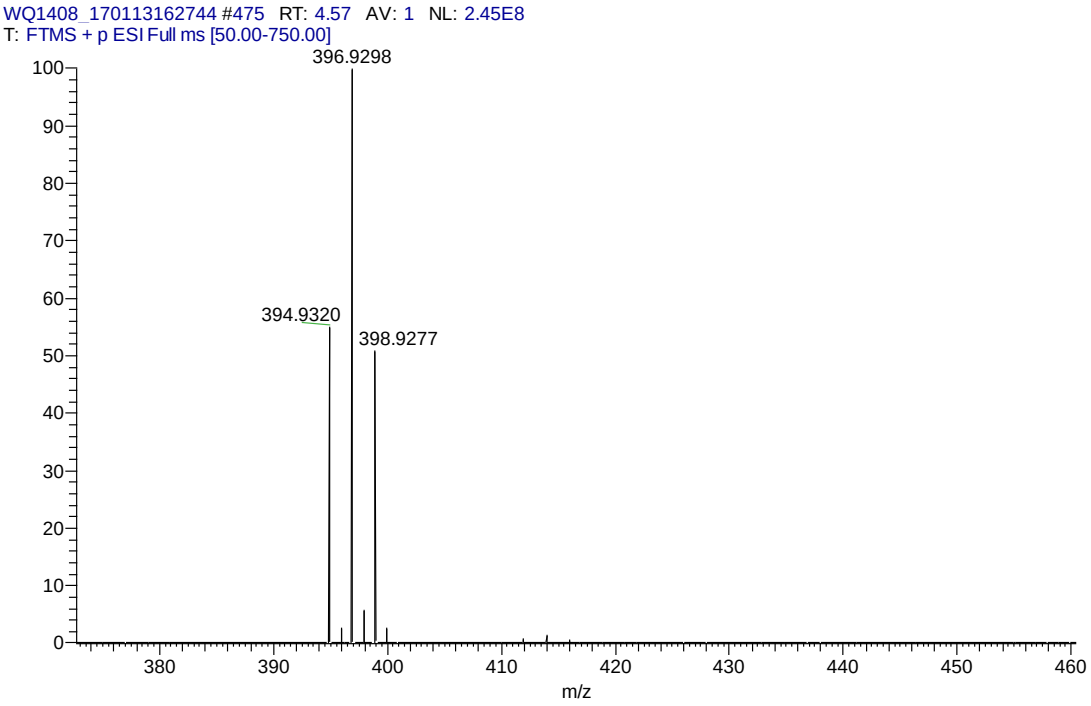

Spectral data of 2f

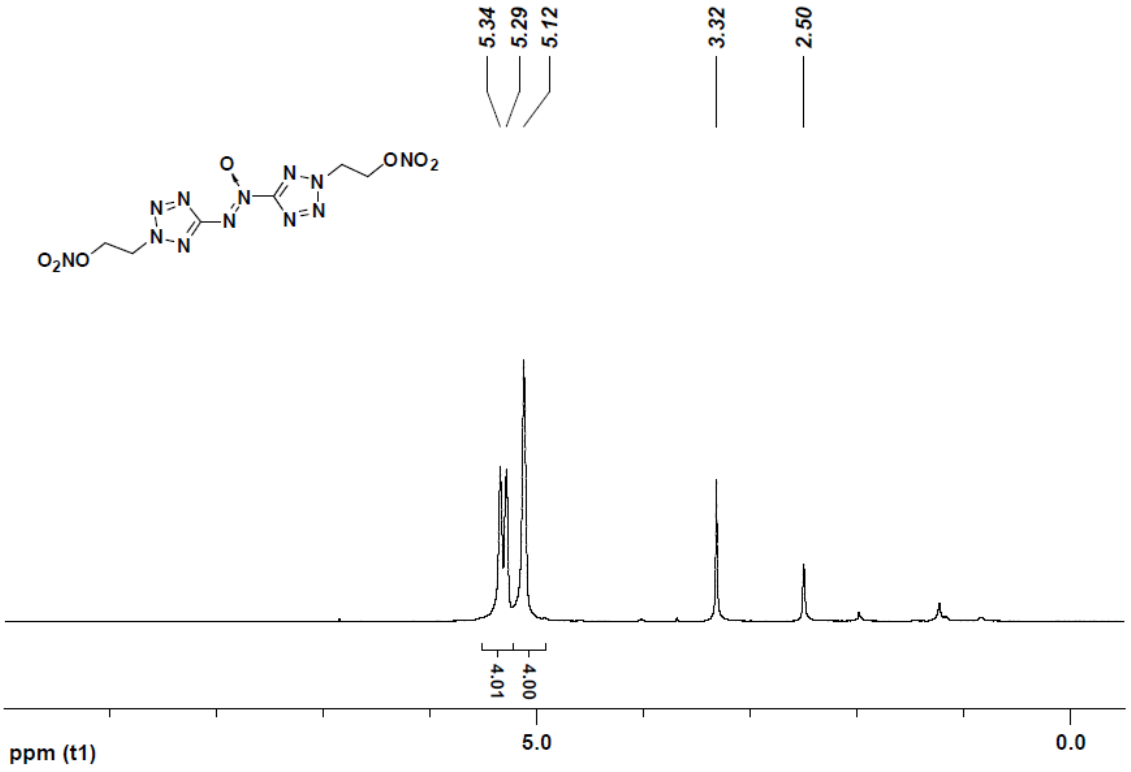

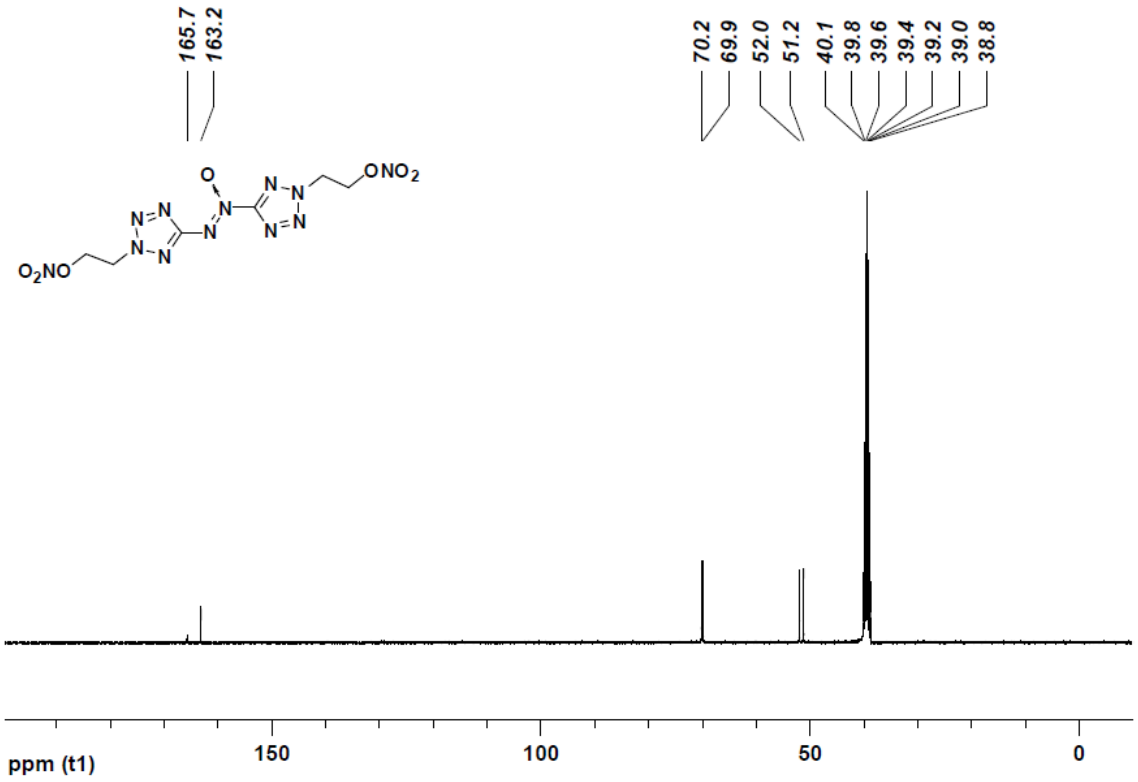

Infrared

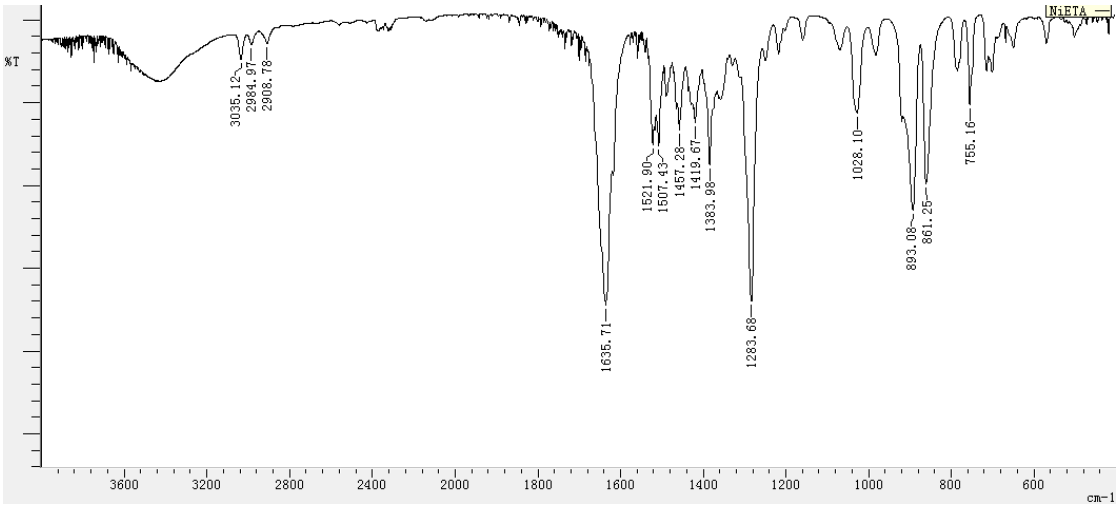

HRMS

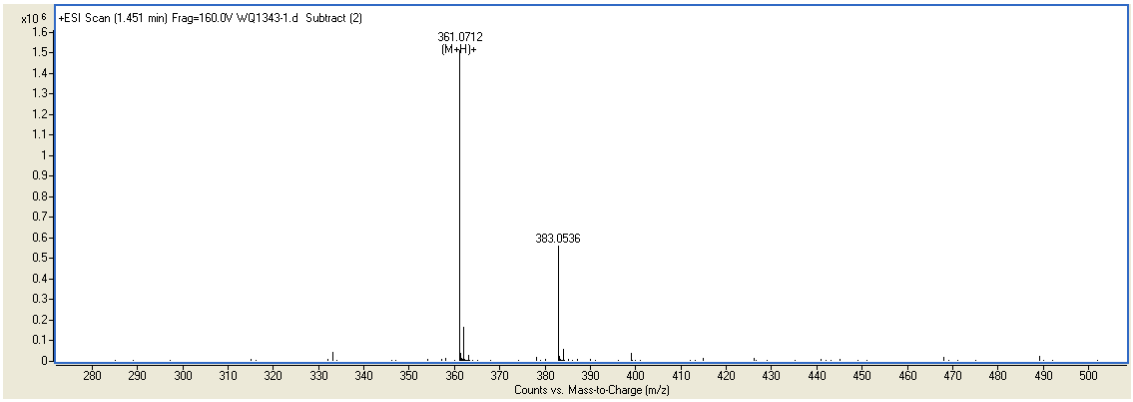

DSC

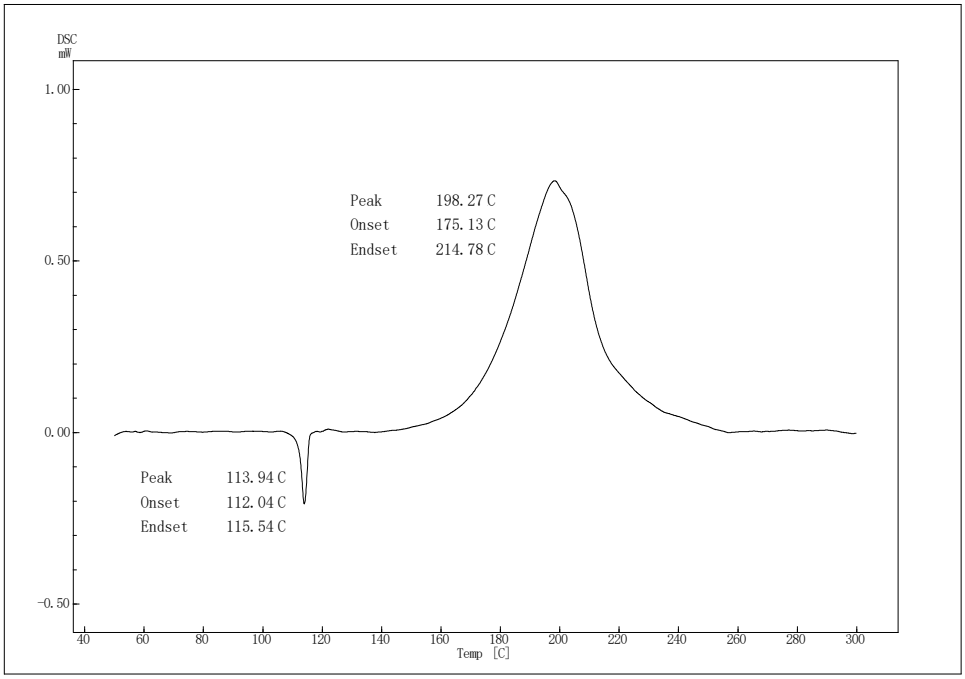

Spectral data of 2g

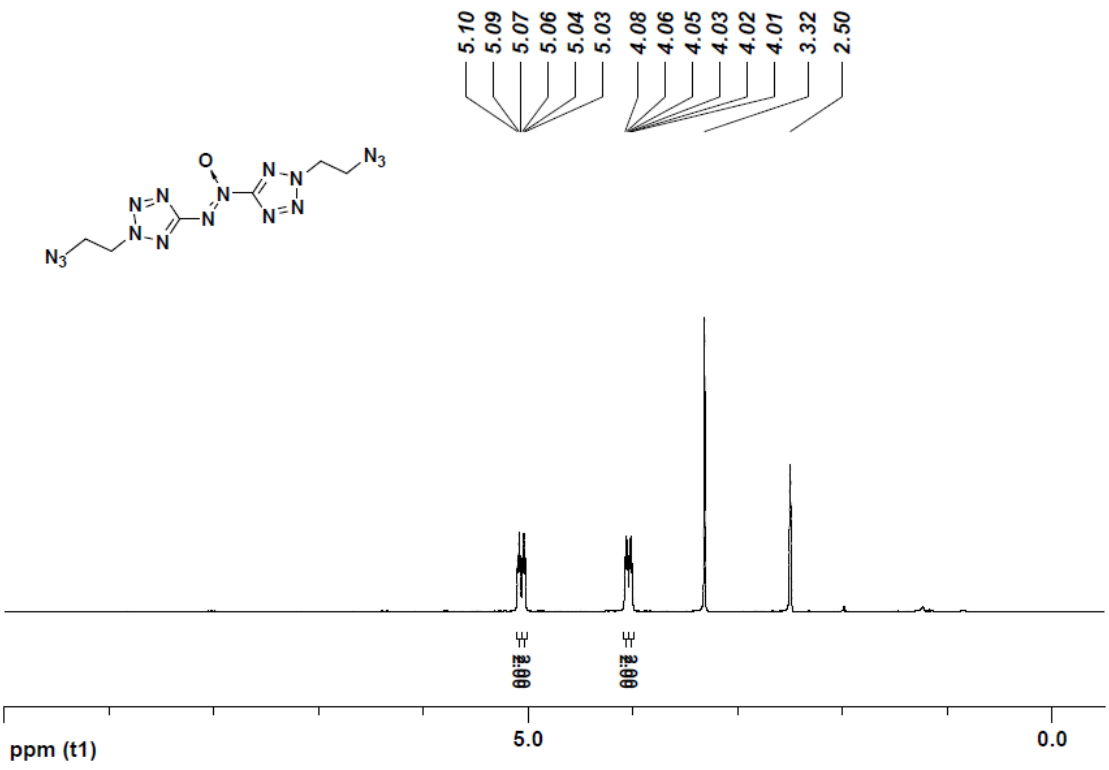

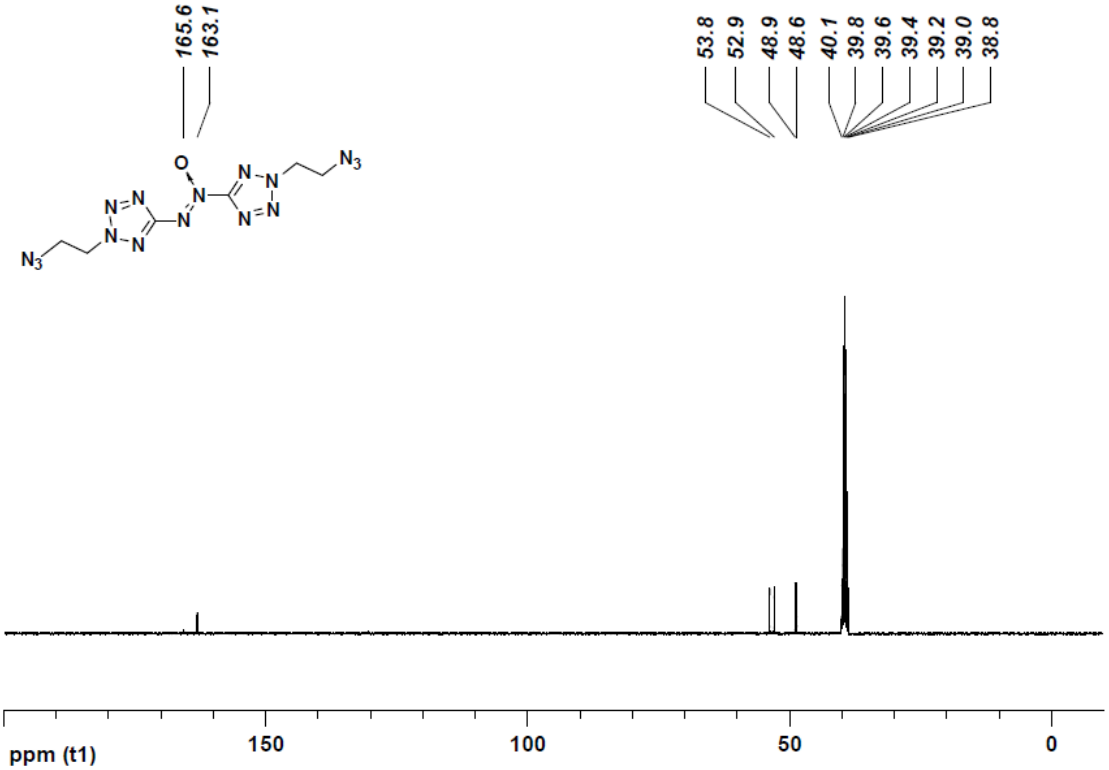

Infrared

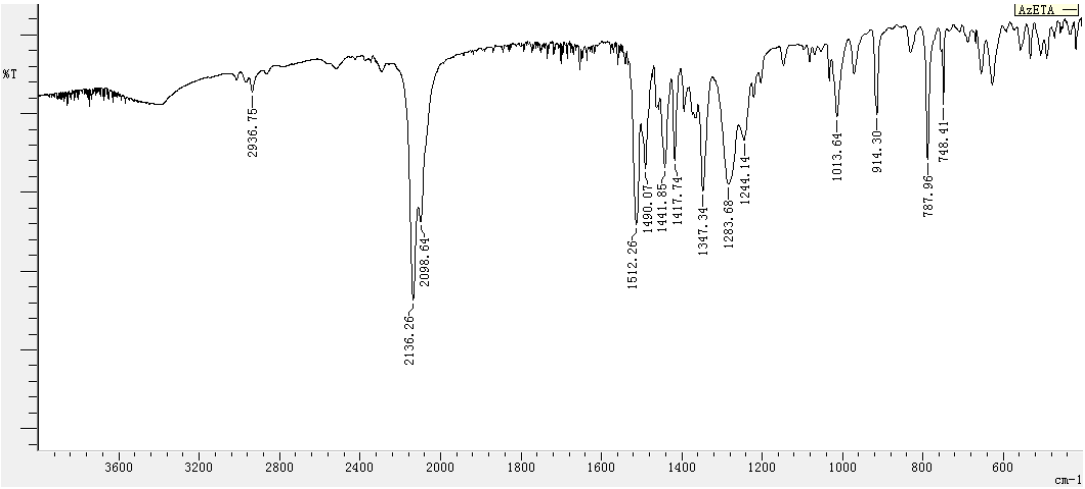

HRMS

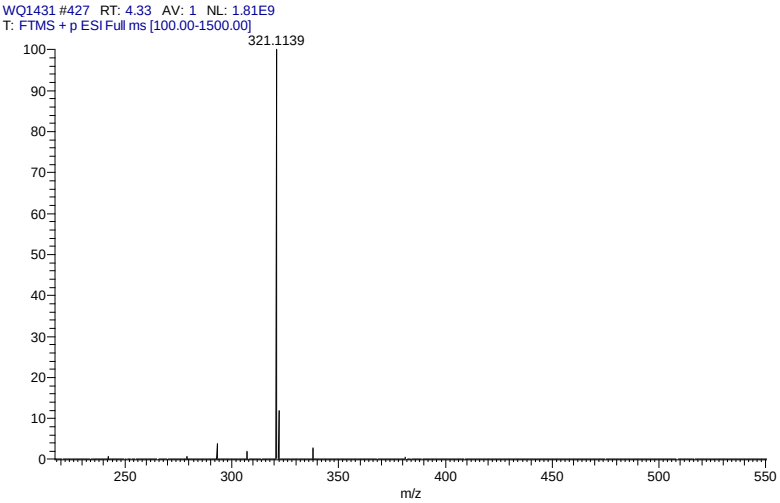

DSC

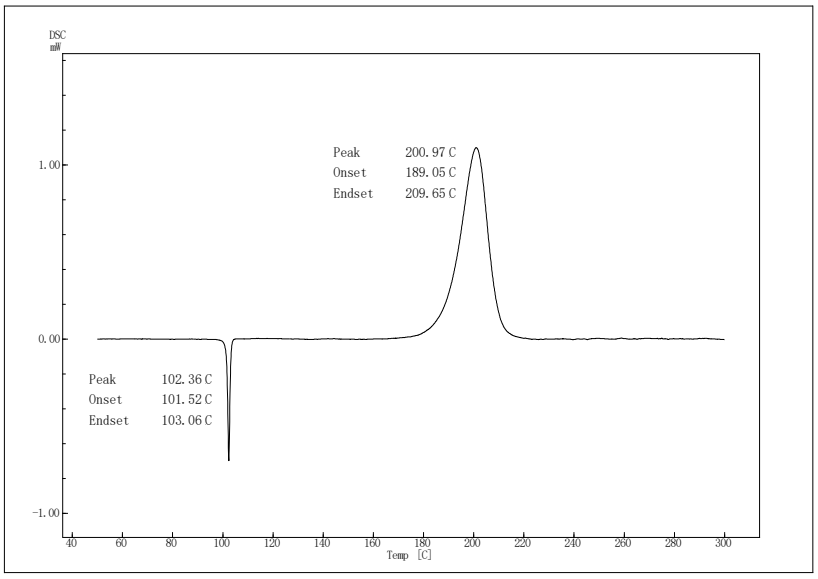

Table S2. Crystal data and structure refinement for **2a**.

Identification code	**2a**
CCDC deposition number	1540159
Empirical formula	C4H6N10O
Formula weight	210.19
Crystal system	Monoclinic
Space group	P21/c
a	7.5607(8) Å
b	13.7150(15) Å
c	8.9269(9) Å
β	102.388(4) °
Z	4
Temperature	299(2) K
Wavelength	0.71073 Å
Calculated density	1.544 g·cm-3
Absorption coefficient	0.123 mm-1
F(000)	432
Crystal size	0.25×0.13×0.06 mm-3
Theta range for data collection	2.76–28.34°
Limiting indices	-10 <= h <= 10, -18 <= k <= 18, -10 <= l <= 11
Reflections unique [Rint]	2219[0.0764]
Data / restraints / parameters	2219/0/138
Goodness-of-fit on F2	1.040
Final R indices [I>2sigma(I)]	R1 = 0.0553, wR2 = 0.1401
R indices (all data)	R1 = 0.0775, wR2 = 0.1562

Table S3. Atomic coordinates and equivalent isotropic displacement parameters ($Å^2$) for **2a**. *U*(eq) is defined as one third of the trace of the orthogonalized U^{ij} tensor.

	x	y	z	*U*(eq)
O(1)	0.2640(2)	0.3622(1)	0.1581(2)	0.061(1)
N(1)	0.4852(2)	0.5059(2)	0.2922(2)	0.043(1)
N(2)	0.5658(2)	0.5923(2)	0.3103(2)	0.042(1)
N(3)	0.5226(2)	0.6502(2)	0.1906(2)	0.047(1)
N(4)	0.4059(2)	0.6006(2)	0.0868(2)	0.045(1)
N(5)	0.2680(2)	0.4377(2)	0.0827(2)	0.039(1)
N(6)	0.1792(2)	0.4588(2)	-0.0506(2)	0.041(1)
N(7)	0.0260(2)	0.2980(2)	-0.0871(2)	0.043(1)
N(8)	-0.0972(2)	0.2708(2)	-0.2087(2)	0.042(1)
N(9)	-0.1389(2)	0.3384(2)	-0.3147(2)	0.049(1)
N(10)	-0.0393(2)	0.4151(1)	-0.2645(2)	0.048(1)
C(1)	0.6887(3)	0.6219(2)	0.4519(3)	0.063(1)
C(2)	0.3870(2)	0.5148(2)	0.1526(2)	0.037(1)
C(3)	0.0597(2)	0.3885(2)	-0.1264(2)	0.038(1)
C(4)	-0.1816(4)	0.1745(2)	-0.2228(3)	0.065(1)

Table S4. Bond lengths [Å] and angles [°] for **2a**.

Bond	Bond length [Å]	Bond	Bond length [Å]
N(5)-O(1)	1.239(2)	N(6)-N(5)	1.268(2)
N(5)-C(2)	1.441(2)	N(6)-C(3)	1.394(2)
N(1)-C(2)	1.312(2)	N(1)-N(2)	1.326(2)
N(2)-N(3)	1.315(2)	N(4)-N(3)	1.323(2)
N(4)-C(2)	1.336(2)	N(2)-C(1)	1.457(3)
N(7)-C(3)	1.329(3)	N(7)-N(8)	1.323(2)
N(9)-N(8)	1.314(2)	N(9)-N(10)	1.315(2)
N(10)-C(3)	1.349(3)	N(8)-C(4)	1.460(3)
C(1)-H(1A)	0.9600	C(1)-H(1A)	0.9600
C(1)-H(1C)	0.9600	C(1)-H(4A)	0.9600
C(4)-H(4B)	0.9600	C(4)-H(4C)	0.9600

Bonds	angle [°]	Bonds	angle [°]
N(5)-N(6)-C(3)	117.1(2)	O(1)-N(5)-N(6)	129.1(2)
O(1)-N(5)-C(2)	117.6(2)	N(6)-N(5)-C(2)	113.2(2)
C(2)-N(1)-N(2)	100.6(2)	N(8)-N(9)-N(10)	106.8(2)
N(8)-N(7)-C(3)	100.8(2)	N(3)-N(4)-C(2)	105.3(2)
N(1)-C(2)-N(4)	114.0(2)	N(1)-C(2)-N(5)	121.1(2)
N(4)-C(2)-N(5)	124.9(2)	N(9)-N(8)-N(7)	114.2(2)
N(9)-N(8)-C(4)	122.9(2)	N(7)-N(8)-C(4)	122.9(2)
N(9)-N(10)-C(3)	105.0(2)	N(7)-C(3)-N(10)	113.2(2)
N(7)-C(3)-N(6)	131.3(2)	N(10)-C(3)-N(6)	115.5(2)
N(3)-N(2)-N(1)	114.4(2)	N(3)-N(2)-C(1)	122.5(2)
N(1)-N(2)-C(1)	123.1(2)	N(2)-N(3)-N(4)	105.7(2)
N(8)-C(4)-H(4A)	109.5	N(8)-C(4)-H(4B)	109.5
H(4A)-C(4)-H(4B)	109.5	N(8)-C(4)-H(4C)	109.5
H(4A)-C(4)-H(4C)	109.5	H(4B)-C(4)-H(4C)	109.5
N(2)-C(1)-H(1A)	109.5	N(2)-C(1)-H(1B)	109.5
H(1A)-C(1)-H(1B)	109.5	N(2)-C(1)-H(1C)	109.5
H(1A)-C(1)-H(1C)	109.5	H(1B)-C(1)-H(1C)	109.5

Table S5. Anisotropic displacement parameters ($Å^2$) for **2a**. The anisotropic displacement factor exponent takes the form: $-2\pi^2[h^2 a^{*2}U^{11} + ... + 2 h k a^* b^* U^{12}]$.

	U^{11}	U^{22}	U^{33}	U^{12}	U^{13}	U^{23}
O(1)	0.088(2)	0.040(1)	0.044(1)	-0.018(1)	-0.011(1)	0.008(1)
N(1)	0.044(1)	0.042(1)	0.041(1)	-0.010(1)	0.007(1)	-0.003(1)
N(2)	0.043(1)	0.044(1)	0.039(1)	-0.012(1)	0.010(1)	-0.005(1)
N(3)	0.054(1)	0.043(1)	0.045(1)	-0.007(1)	0.014(1)	-0.001(1)
N(4)	0.047(1)	0.044(1)	0.042(1)	-0.001(1)	0.006(1)	-0.002(1)
N(5)	0.044(1)	0.036(1)	0.037(1)	0.003(1)	0.010(1)	0.001(1)
N(6)	0.040(1)	0.044(1)	0.039(1)	0.002(1)	0.006(1)	0.001(1)
N(7)	0.042(1)	0.041 (1)	0.040(1)	0.000(1)	-0.002(1)	-0.008(1)
N(8)	0.042(1)	0.044(1)	0.036(1)	0.000(1)	0.002(1)	-0.010(1)
N(9)	0.050(1)	0.059(2)	0.037(1)	0.002(1)	0.006 (1)	-0.004(1)
N(10)	0.049(1)	0.054(1)	0.040(1)	0.000(1)	0.007(1)	0.001(1)
C(1)	0.068(2)	0.073(2)	0.044(2)	-0.032(2)	0.001(2)	-0.007(2)
C(2)	0.035(1)	0.038(1)	0.038(1)	0.001(1)	0.010(1)	-0.005(1)
C(3)	0.033(1)	0.040(1)	0.041(1)	0.004(1)	0.010(1)	-0.007(1)
C(4)	0.077(2)	0.050(2)	0.059(2)	-0.016(2)	-0.005(2)	-0.014(2)

Table S6. Torsion angles [°] for **2a**.

Bonds	Torsion angle [°]	Bonds	Torsion angle [°]
C(3)-N(6)-N(5)-O(1)	-0.4(3)	C(3)-N(6)-N(5)-C(2)	-179.6(2)
N(2)-N(1)-C(2)-N(4)	0.5(2)	N(2)-N(1)-C(2)-N(5)	-178.0(2)
N(3)-N(4)-C(2)-N(1)	-0.3(2)	N(3)-N(4)-C(2)-N(5)	178.2(2)
O(1)-N(5)-C(2)-N(1)	-1.2(3)	N(6)-N(5)-C(2)-N(1)	178.1(2)
O(1)-N(5)-C(2)-N(4)	-179.6(2)	N(6)-N(5)-C(2)-N(4)	-0.3(2)
N(10)-N(9)-N(8)-N(7)	0.5(2)	N(10)-N(9)-N(8)-C(4)	179.6(2)
C(3)-N(7)-N(8)-N(9)	-0.6(2)	C(3)-N(7)-N(8)-C(4)	-179.7(2)
N(8)-N(9)-N(10)-C(3)	-0.1(2)	N(8)-N(7)-C(3)-N(10)	0.5(2)
N(8)-N(7)-C(3)-N(6)	-179.0(2)	N(9)-N(10)-C(3)-N(7)	-0.2(2)
N(9)-N(10)-C(3)-N(6)	179.3(2)	N(5)-N(6)-C(3)-N(7)	-3.8(3)
N(5)-N(6)-C(3)-N(10)	176.8(2)	C(2)-N(1)-N(2)-N(3)	-0.5(2)
C(2)-N(1)-N(2)-C(1)	177.9(2)	N(1)-N(2)-N(3)-N(4)	0.4(2)
C(1)-N(2)-N(3)-N(4)	-178.1 (2)	C(2)-N(4)-N(3)-N(2)	0.0(2)

Computation details

The heats of formation of **2a**, **2c**, **2f**, **2g** were carried out by using the Gaussian09 (Revision B.01) suite of programs based on isodesmic reactions (Scheme S2).[4] The elementary geometric optimization and the frequency analysis were performed at the level of B3LYP/6-311+G**. The total energy was performed at the level of MP2/6-311++G**.

Scheme S2. Isodesmic reactions for the calculation of heats of formation.

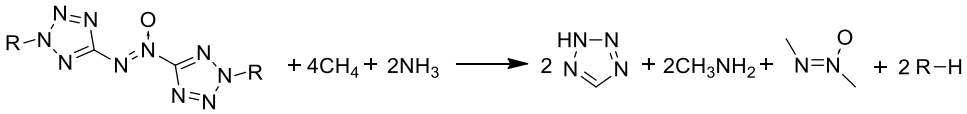

Table S7. Calculated (B3LYP/6-31+G**//MP2/6-311++G**) total energy (E_0), Zero-Point Energy (ZPE), values of thermal correction (H_T), and heats of formation (HOF) of **2a**, **2c**, **2f**, **2g**.

Compound	E_0 (hartree)	ZPE (hartree)	H_{corr} (hartree)	HOF (kJ·mol^{-1})
2a	-777.0625142	0.144634	0.157615	519.8
2c	-961.1717590	0.141439	0.156798	869.0
2f	-1413.9153692	0.216076	0.239300	345.4
2g	-1182.0796277	0.208876	0.230536	682.3
2*H*-Tetrazole	-257.7068416	0.047597	0.051961	318.2
$CH_3N{=}N(O)CH_3$	-263.9193653	0.090010	0.095983	50.6
CH_4	-40.3969989	0.044793	0.048605	-74.4
NH_3	-56.4270341	0.034372	0.038190	-46.0
CH_3NH_2	-95.6223961	0.064026	0.068401	-22.5
CH_3CN	-132.4579378	0.045279	0.049840	87.9
C_2H_6	-79.6059746	0.074599	0.079027	-84.7
CH_3ONO_2	-319.6038874	0.054263	0.060193	-120.5
CH_3N_3	-203.5906456	0.049792	0.054130	293.9

References

4 M. J. Frisch, et al.,G. W. Trucks, H. B. Schlegel, G. E. Scuseria, M. A. Robb, J. R. Cheeseman, G. Scalmani, V. Barone, B. Mennucci, G. A. Petersson, H. Nakatsuji, M. Caricato, X. Li, H. P. Hratchian, A. F. Izmaylov, J. Bloino, G. Zheng, J. L. Sonnenberg, M. Hada, M. Ehara, K. Toyota, R. Fukuda, J. Hasegawa, M. Ishida, T. Nakajima, Y. Honda, O. Kitao, H. Nakai, T. Vreven, J. A. Montgomery, Jr., J. E. Peralta, F. Ogliaro, M. Bearpark, J. J. Heyd, E. Brothers, K. N. Kudin, V. N. Staroverov, R. Kobayashi, J. Normand, K. Raghavachari, A. Rendell, J. C. Burant, S. S. Iyengar, J. Tomasi, M. Cossi, N. Rega, J. M. Millam, M. Klene, J. E. Knox, J. B. Cross, V. Bakken, C. Adamo, J. Jaramillo, R. Gomperts, R. E. Stratmann, O. Yazyev, A. J. Austin, R. Cammi, C. Pomelli, J. W. Ochterski, R. L. Martin, K. Morokuma, V. G. Zakrzewski, G. A. Voth, P. Salvador, J. J. Dannenberg, S. Dapprich, A. D. Daniels, Ö. Farkas, J. B. Foresman, J. V. Ortiz, J. Cioslowski, D. J. Fox, *Gaussian 09, Revision B.01*, Gaussian, Inc., Wallingford CT, **2009**.